

# A novel three-phase switched capacitor multilevel inverter for PV applications

---

Received: 5 January 2026

---

Accepted: 19 May 2026

---

Published online: 27 May 2026

---

Cite this article as: Nayak N., Krishna A.M., Jena K. *et al.* A novel three-phase switched capacitor multilevel inverter for PV applications. *Sci Rep* (2026). <https://doi.org/10.1038/s41598-026-54408-0>

---

Narayan Nayak, A. Murali Krishna, Kasinath Jena, Krishna Kumar Gupta, Dhananjay Kumar & Niraj Kumar Dewangan

---

We are providing an unedited version of this manuscript to give early access to its findings. Before final publication, the manuscript will undergo further editing. Please note there may be errors present which affect the content, and all legal disclaimers apply.

If this paper is publishing under a Transparent Peer Review model then Peer Review reports will publish with the final article.

ARTICLE IN PRESS

# A Novel Three-Phase Switched Capacitor Multilevel Inverter for PV Applications

Narayan Nayak<sup>1</sup>, A. Murali Krishna<sup>2</sup>, Kasinath Jena<sup>3</sup>, Krishna Kumar Gupta<sup>4</sup>, Dhananjay Kumar<sup>5</sup>, Niraj kumar Dewangan<sup>6\*</sup>

<sup>1,3</sup>Department of Electrical and Electronics Engineering, ARKA JAIN University, India

Email:kasi.jena@gmail.com, Email: nayaknarayan111@gmail.com

<sup>2</sup>Department of Electronics and Communications Engineering, KL University, AP, India

muralikrishna.annaldas@gmail.com

<sup>4</sup>Department of Electrical and Instrumentation Engineering, Thapar Institute of Engineering & Technology, Patiala, India

Email: kkg.manit@gmail.com

<sup>5</sup>Department of Electrical Engineering, Government Engineering College Siwan, Bihar, India

Email: dhananjaymanit23@gmail.com

<sup>6\*</sup>Manipal Institute of Technology, Manipal Academy of Higher Education, Manipal, India

Corresponding Author: Niraj Kumar Dewangan,  
niraj.dewangan@manipal.edu\*

## Abstract

This article introduces a new, compact 3- $\phi$ , 5-level (line-to-line) switched-capacitor multilevel inverter (5L-SCMLI) design. This design can automatically balance its capacitor voltages and offers a way to increase its voltage gain. There is no extra magnetic circuit or DC-DC boost converter needed to accomplish a voltage gain of two in the proposed topology (PT). The PT is more efficient and cost-effective since it synthesizes 5-levels (line-to-line) using only five switches, two capacitors and one diode. A detailed comparison with current SCMLI structures shows the PT benefits. The extensive simulation and experimental studies have been conducted to validate the PT effectiveness and assess the efficacy of the proposed technique. The PT stands out as the most cost-effective design at only 54.59 USD with an efficiency 97.81%. This work aligns with SDG 7 (Affordable and Clean Energy) and SDG 9 (Industry, Innovation and Infrastructure) by proposing a cost-

effective, high-efficiency multilevel inverter that enhances energy conversion and supports sustainable power electronics systems.

**Keywords:** Cost function, Multilevel Inverter, Switched Capacitors, LS-PWM, Switch Count, total Voltage Stress, SDG 7, SDG 9.

## I. Introduction

Renewable energy has emerged as the most promising alternative to fossil fuels amid their depletion. Nonetheless, although most renewable sources are DC, alternating current (AC) is necessary for domestic and industrial applications. Power electrical devices, such as inverters, are utilised to facilitate efficient DC-to-AC conversion, thereby bridging this gap[1]. Conventional two-level inverters are widely used but face significant drawbacks, including high switching losses and inferior harmonic performance. Multilevel inverters (MLIs) have attained considerable prominence in the power electronics domain owing to their benefits over traditional inverters, such as reduced  $dv/dt$ , enhanced power quality, and reduced total harmonic distortion (THD), minimizing voltage stress on power devices. Due to these advantages, MLIs are widely utilised in diverse applications, including flexible AC transmission systems (FACTS), active power filters, and renewable energy generation (REG) [2]. However, incorporating an inductor in a boost converter increases the system's size and complicates its control architecture. A feasible design for medium- and high-power applications is the SCMLI. It can boost voltage, reduce the number of devices, and naturally balance capacitor voltage without the need for extra sensors or controllers. Several five-level inverter configurations employing switched-capacitor (SC) technology have been presented in the literature, each offering distinct advantages and limitations. A dual-T-type 5-level SCMLI that uses a half bridge to twice the voltage. It deals with the impulse charging currents and uneven operation that are frequent in SCMLI [3]. Using only eight switches and two capacitors, this five-level common ground inverter efficiently boosts voltage twice. It minimises leakage current, balances capacitor voltages, and achieves high efficiency (~96.5%). [4]. A common ground type inverter that uses SC to boost voltage while cutting down the energy those capacitors need to store. Unlike older designs where capacitors had to handle peak output voltage, this one uses capacitors rated just for half that voltage. It balances voltage on its own, keeps voltage change rates low, and doesn't need sensors to operate [5]. It introduces an H-9 topology with nine switches for output voltage control. Uses virtual grounding to cut down leakage current and keeps the capacitor ripple balanced [6]. A new five-level inverter design focuses on a common ground design to minimise leakage current. The inverter uses just two SC, each rated for half the output voltage, which cuts down the size, cost, and complexity [7]. An improved five-level ANPC inverter, unlike the conventional version that utilises only half of the DC-link voltage, achieves doubled DC voltage utilisation by employing an SC charged to half of the input voltage [8]. A single-phase five-level SC boost inverter is proposed to achieve higher voltage gain compared to conventional impedance-source inverters. The SC configuration effectively doubles the boosting capability while ensuring self-balancing of capacitor voltages [9-11]. A novel dual-mode, transformerless five-level inverter with a common-ground architecture for PV grid-connected systems. The topology provides efficient voltage boosting and self-balancing, significantly reduces leakage current, and ensures stable power injection with simple control strategies, thereby improving reliability, power quality, and adaptability to input voltage variations [12-14]. A five-level inverter that

addresses the problem of current spikes by employing a soft-charging technique using a dedicated inductor-switch circuit. The topology enhances voltage gain and achieves improved utilisation of the dc-link voltage compared to conventional designs [15-17]. A single-phase five-level converter design using SCs. The key point is that it boosts voltage without the usual H-bridge for reversing polarity, which reduces switching losses and voltage stress on parts [18-19]. A new single-phase five-level SC boost inverter with improved voltage gain over traditional impedance-source inverters. It uses an SC structure that doubles the boost factor while keeping capacitor voltages balanced [20-21].

The main benefits of the suggested topology are as follows:

- (i) Increasing boosting ability, i.e, 2X
- (ii) Natural balancing of the capacitor voltage
- (iii) Lower total standing voltage(TSV)
- (iv) Lower cost
- (v) Only half of the switches operate for any voltage level.
- (vi) Low losses
- (vii) Operate for a wide range of power factors

The remaining details of the section are as follows: Part II specifies the SCMLI design's concept and operation. In Section III, discuss the PT control techniques. The idea of power loss of the proposed **5L-SCMLI** is explained in detail in Section IV. Section V covered a comparison study to establish the effectiveness of the suggested topology. In part VI, explore the analysis of results. The last section, VII, provides a summary of the work.

## II. Proposed 5L-SC-MLI Topology

### (a) Proposed Three-Phase 5L-SC-MLI Topology

Figure 1(a) illustrates a three-phase 5L-SCMLI configuration that employs a single input source and comprises five switches, two capacitors, and two diodes. The PT generates five different voltage levels (line to line )as an output:  $2V_{DC}$ ,  $1V_{DC}$ ,  $0$ ,  $-1V_{DC}$ , and  $-2V_{DC}$ . The PT doesn't need any sensor or any other circuit to keep the capacitor voltage balanced. The capacitors naturally keep themselves balanced because they are connected to the input source in both series and parallel[18][19][26]. Table 1 shows the order in which the proposed topology operated for each state of the pole voltage  $v_{RO}$  for phase R (refer to Fig. 1(b)). Voltage stress for different voltages is noted in Table 2.

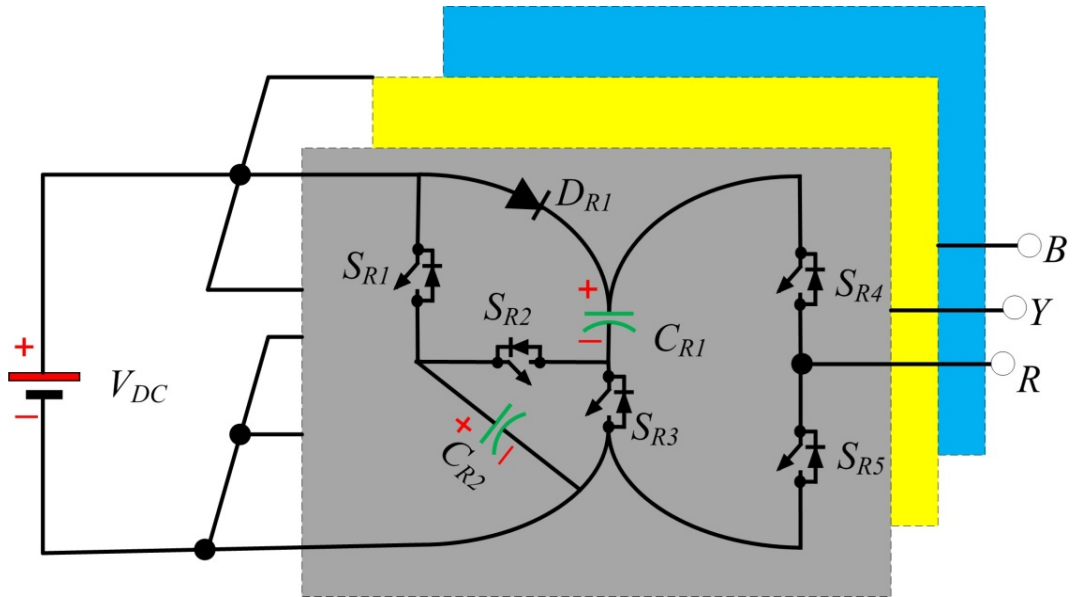


Fig.1(a) Proposed 5-level Three phase Topology

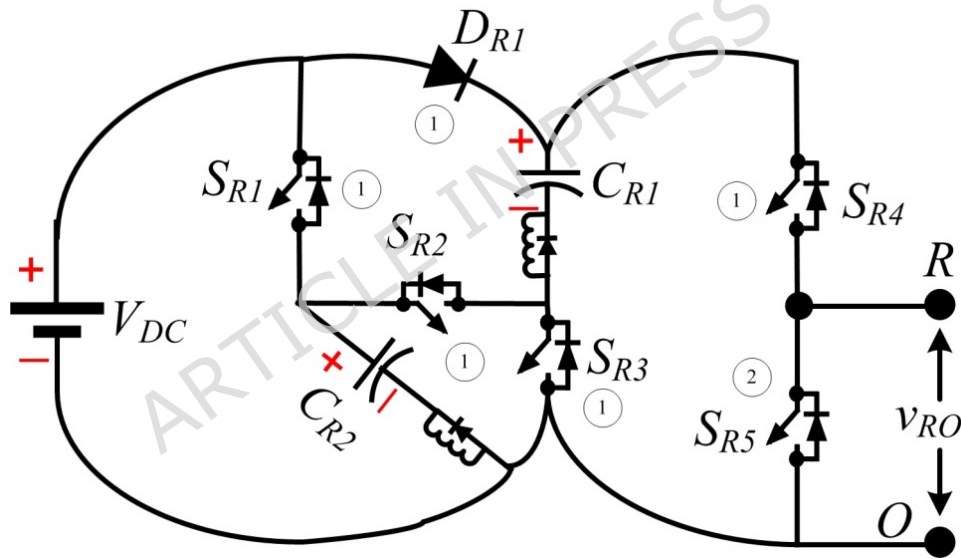


Fig.1 (b) R-Phase

Table 1: Switching pattern of 5L-SC-MLI

Mode	$S_{R1}$	$S_{R2}$	$S_{R3}$	$S_{R4}$	$S_{R5}$	$C_{R1}$	$C_{R2}$	$v_{RO}$
$\beta_1$	1	-	-	-	1	-	C	0
$\beta_2$	-	-	1	1	-	C	-	$1V_{DC}$
$\beta_3$	-	1	-	1	-	D	D	$2V_{DC}$

A:state, "1": Active-state, "-": inactive state, C: charging,D: discharging,  $v_{RO}$ : output

**Table 2:Voltage stress of 5L-SC-MLI**

Mode	$S_{R1}$	$S_{R2}$	$S_{R3}$	$S_{R4}$	$S_{R5}$	$v_{RO}$
$\beta_1$	0	$1V_{DC}$	$1V_{DC}$	$1V_{DC}$	0	0
$\beta_2$	$1V_{DC}$	$1V_{DC}$	0	0	$1V_{DC}$	$1V_{DC}$
$\beta_3$	$1V_{DC}$	0	$1V_{DC}$	0	$2V_{DC}$	$2V_{DC}$

**(b) Proposed Three Phase 5L-SC-MLI Topology operation**

**Mode - $\rho_1$ :  $v_{RO}=0$**

$v_{RO}=0$  can be generated by activating  $S_{R5}$  simultaneously  $S_{R1}$  activated to charge  $C_{R2}$  to  $V_{dc}$  as illustrated in Fig. 2(a). The pole voltage and the capacitor charging path are indicated by blue and red dotted lines, respectively.

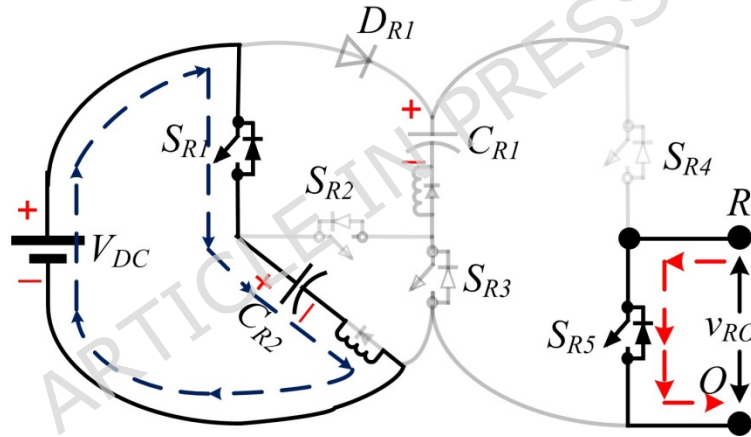


**Fig.2(a)  $v_{RO} = 0$**

**Mode - $\rho_2$ :  $v_{RO}=V_{dc}$**

$v_{RO}=V_{dc}$  can be generated by activating  $S_{R4}$  simultaneously  $S_{R3}$  activated to charge  $C_{R1}$  to  $V_{dc}$  as illustrated in Fig. 2(b).

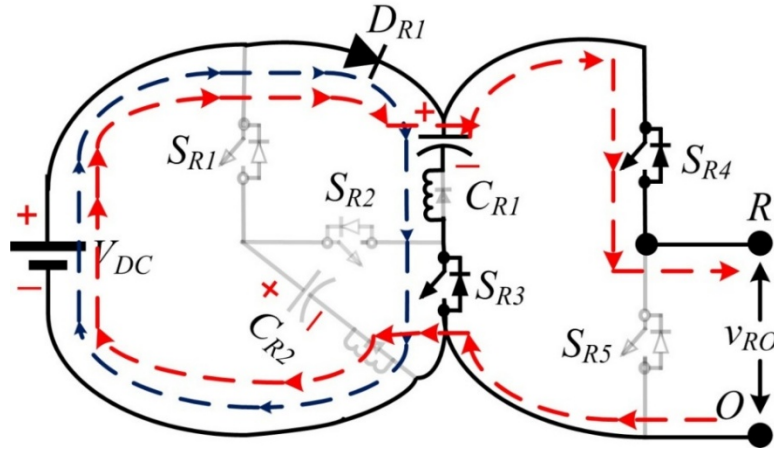


**Fig.2 (b)**  $v_{RO} = V_{dc}$

**Mode -p<sub>2</sub>:**  $v_{RO} = 2V_{dc}$

$v_{RO} = 2V_{dc}$  can be generated by activating  $S_{R4}$  and  $S_{R2}$ , here both  $C_{R1}$  and  $C_{R2}$  discharges through load as illustrated in Fig. 2(c).

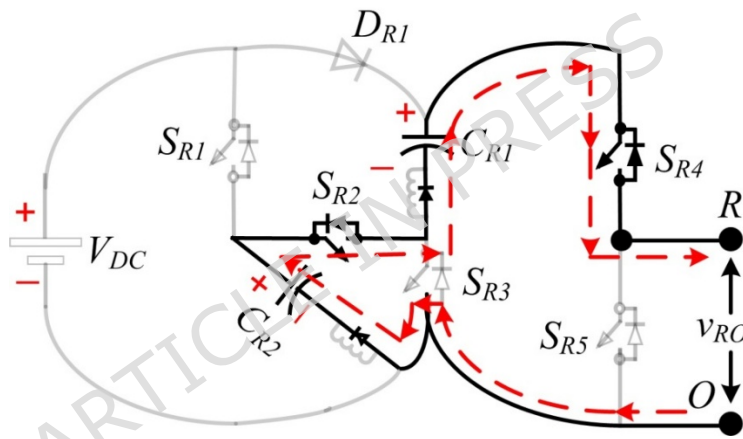


**Fig.2 (c)**  $v_{RO} = 2V_{dc}$

**Fig.2 (a)**  $v_{RO} = 0$  (b)  $v_{RO} = V_{dc}$  (c)  $v_{RO} = 2V_{dc}$

**(c) Modular Structure of the PT**

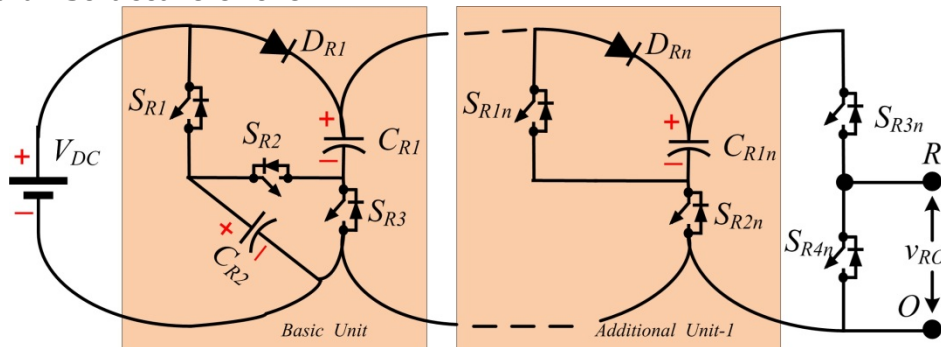


**Fig 2(d) Modular structure of the PT**

The modular structure for the PT are as shown in the Fig.2(d). For the basic unit it generates 3-level pole voltage and 5-level line voltage. For "n" additional unit pole voltage level =  $n + 3$

$$\begin{aligned} \text{line voltage} &= 7 + (n - 1)2 \\ N_{\text{sw}} &= 7 + (n - 1)2 \\ N_c &= 2 + n \\ N_d &= 1 + n \end{aligned}$$

### III. Control Method

The PT has been designed to produce 3-Level output waveforms using a Level-Shifted pulse width modulation (LSPWM) technique to create gate pulses[18][22][26]. The control technique of the PT is depicted in Fig. 3. In this proposed PWM scheme, two carrier signals ( $A_c$ )  $C_1(t)$  and  $C_2(t)$ , per phase at the desired switching frequency is compared with a modulating signal ( $U_a$ ) for the R-Phase. The outputs of the comparators are added to get the aggregated signals  $a(t)$ . This aggregated signal  $a(t)$  is mapped to the output level, as shown in Table 1, to obtain the switching pulse for Phase R. Similarly, the switching pulses for Phase -Y and Phase -B can be obtained.

$$M = \frac{U_r}{2A_c}$$

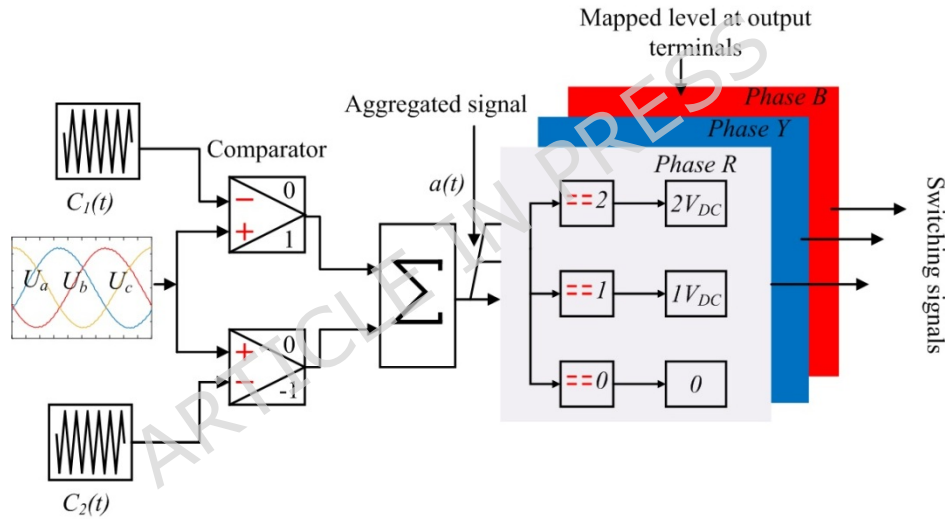


**Fig.3** Modulation Scheme

#### Selection of capacitance

The typical relationship between voltage ripple ( $\delta V$ ) across a capacitor and capacitance is inversely proportional. The values of  $t_1$ ,  $t_2$ , can be calculated from Fig.4 as[26]

$$t_1 = \frac{\sin(\frac{1}{2})}{2\pi f} \quad (1)$$

$$t_2 = \frac{\pi - \sin(\frac{1}{2})}{2\pi f} \quad (2)$$

Capacitance values are derived from the maximum load current and the longest discharge period of the capacitor. Therefore, the maximum discharge of a capacitor can be represented as follows:

$$Q_{C,i} = \int_x^{t_y} I_m \sin(\omega t - \phi) dt \quad (3)$$

Hence, the optimum capacitance values can be determined by:

$$C_i > \frac{Q_{C,i}}{\delta V \times V_{dc}} \quad (4)$$

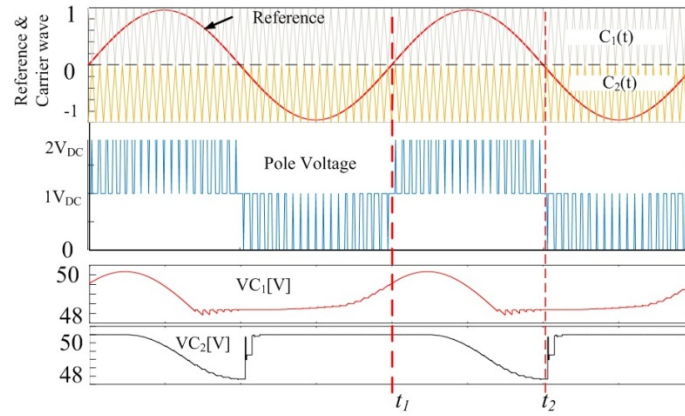


**Fig. 4:** Capacitor discharging instant

Figure 5(a) and (b) show the least amount of capacitance  $C_1$  and  $C_2$  needed for resistive and inductive loads. It is noted that the capacitance required for a resistive load exceeds that for an inductive load when the voltage ripples are equal.

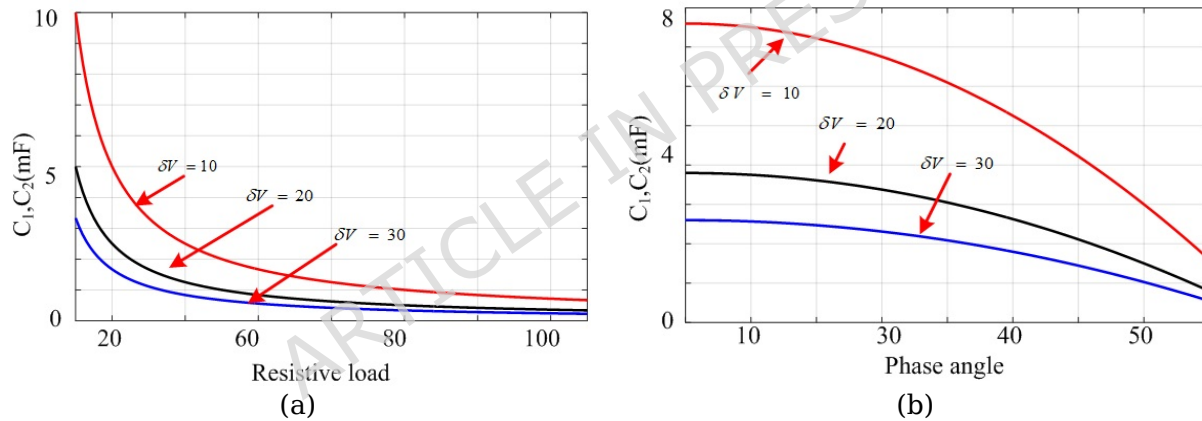


Fig.5 (a) Resistive load, (b) Inductive load with different p.f

#### IV. Losses analysis of the proposed SCMLI

There are a total of three kinds of losses in an SCMLI: switching losses ( $P_S$ ), capacitor losses ( $P_r$ ), and conduction losses ( $P_C$ ). Power switches and diodes are the sources of conduction and switching losses, whereas capacitors are the sources of ripple losses.

##### Conduction losses ( $P_C$ ):

The on-state of semiconductor devices causes these losses [12].

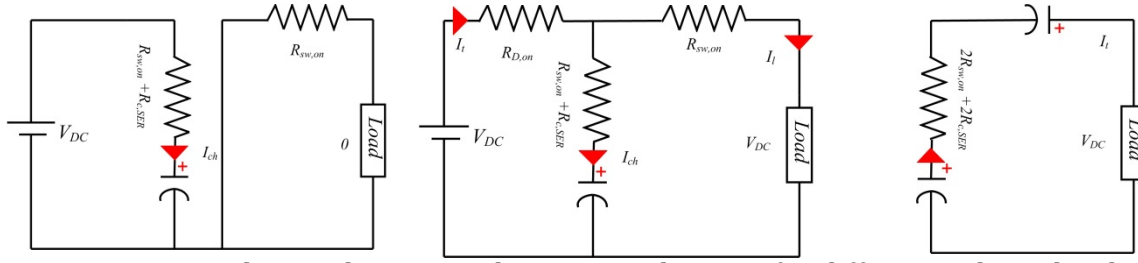


**Fig.6** Conduction loss equivalent circuit diagram for different voltage levels

Fig. 6 demonstrates the way to express the instantaneous conduction losses for a resistive load as follows[27]:

$$P_{i,1} = I_{ch}^2 (R_{sw,on} + R_{c,SER}) \quad (4)$$

$$P_{i,2} = I_{ch}^2 (R_{sw,on} + R_{c,SER} + R_{D,on}) + I_l^2 (R_{sw,on}) + I_l^2 (R_{D,on}) \quad (5)$$

$$P_{i,2} = I_{ch}^2 (R_{sw,on} + R_{c,SER} + R_{D,on}) + I_l^2 (R_{sw,on}) \quad (6)$$

Where  $I_t = I_l + I_{ch}$

$$P_{avg,1} = \frac{t_1}{T} P_{i,1} \quad (7)$$

$$P_{avg,2} = \frac{2(t_2 - t_1)}{T} P_{i,2} \quad (8)$$

The conduction losses can be calculated as

$$P_C = \sum_{i=1}^3 P_{avg,i} \quad (9)$$

### Switching losses ( $P_S$ ):

These losses arise during the switching transitions of semiconductor devices. The corresponding loss can be expressed as[12][15]

$$P_S = \frac{1}{2} V_{off} f_{sw}(t) [t_{on} + t_{off}] \quad (10)$$

$V_{off}$ : off-state voltage,  $t_{on}$  and  $t_{off}$ : on and off time durations of the switch.

### Capacitor losses ( $P_{rip}$ ):

The variation in capacitor voltage during the discharging process leads to ripple losses.

$$\delta V = \frac{1}{C_i} \int_{t_x}^{t_y} i_{C,i} dt \quad (11)$$

$$P_{rip} = \frac{f}{2} C_i \delta V^2 \quad (12)$$

$\delta V$ : Ripple voltage,  $(t_x, t_y)$ : discharging time span,  $i_{C,i}$ : Current flowing through the capacitor

The total power loss can be expressed as:

$$P_{total} = \sum P_C + \sum P_S + \sum P_{rip} \quad (13)$$



Switch	IXTP36N30T(TO220), 300V, 36A	2.65	3	6	12	3	5	1	10	3
	IRFP460PBF (TO247), 500V, 20A	4.11	4	3	-	4	4	7	2	2
Diode	SBR40U300CTB, 300V, 40A	2.11	3	1	2	4	-	1	-	1
	RURU5050(TO-218), 500V, 50V	3.1	-	1	-	-	-	-	-	-
Capacitor	871-B43415C3218A000, 2100 $\mu$ F, 300V	13.83	2	2	2	2	2	1	2	2
	ALF70G222KP500, 2200 $\mu$ F, 500V	26.17	-	1	-	-	-	2	-	-
Drive	TLP250, 25kHz	2.18	7	9	12	7	9	8	12	5
Total cost(\$>@700W			75.7	128	89.8	75.7	77.9	177	88.5	54.59

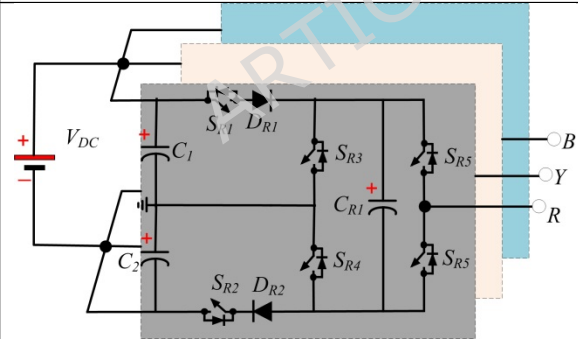
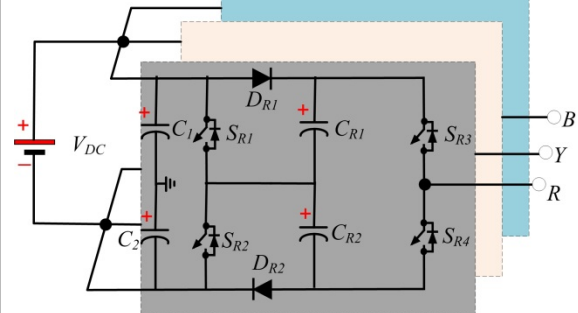
\*www.mouser.in

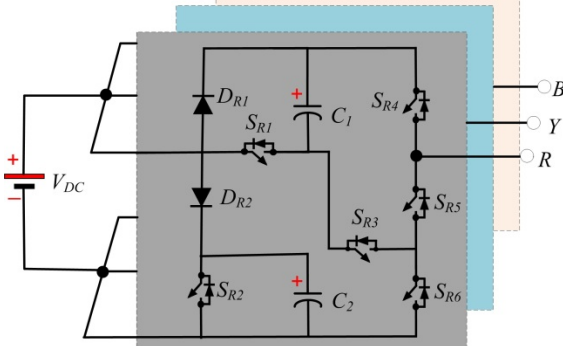
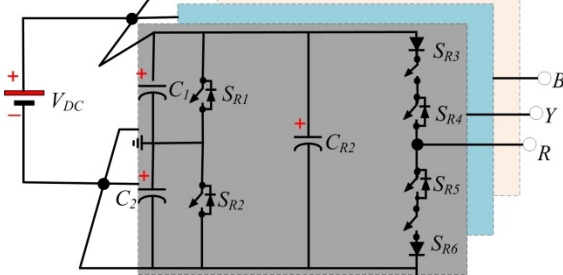
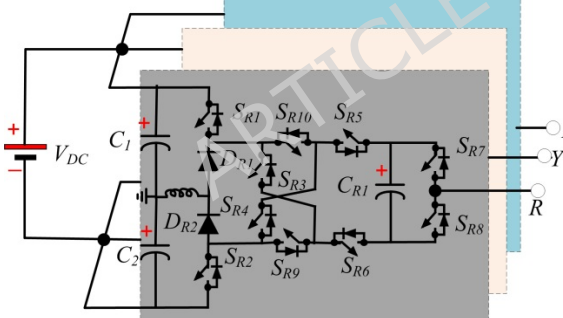
**Table 4: Comparative analysis with the existing Topologies**

Parameter	[3]	[4]	[10]	[6]	[13]	[17]	[11]	[14]	[15]	[20]	[19]	[18]	[PT]
a	10	4	9	9	7	8	12	7	9	4	6	7	5
b	1	1	2	1	4	1	2	3	-	2	2	-	1
c	1	1	3	2	2	2	2	2	2	4	3	1	2
d	2	2	2	2	2	2	1.5	2	2	2	1	2	2
e	14	5	15	14	16	15	11	14	9	6	5	7	7
f	2	2	2	2	2	2	2	2	2	1.5	1	2	2
g	10	4	9	9	7	8	12	7	9	4	6	7	5

a. No. of switches, b. No. of diodes/inductor, c. No. of capacitors, d. MBV, e. TSV, f. Gain, g=No.driver

**Table 5. Merist and Key Features of the 3 Phase SCMLI Topologies**

Ref.	Topologies	Metiers	Key features and Remarks
[25]		$N_{comp} = 11$ $TSV_{pu}/leve = 2$ $gain = 1$ $T_{SC,M} = 1$ $\eta = 96.8\% @ 700$ W	<ul style="list-style-type: none"> <li>□ Can not generate any level operation under open-circuit fault condition of the capacitor.</li> <li>□ larger energy storage requirement.</li> </ul>
[20]		$N_{comp} = 14$ $TSV_{pu}/leve = 2$ $gain = 1,5$ $T_{SC,M} = 1$ $\eta = 96.2\% @ 700$ W	<ul style="list-style-type: none"> <li>□ Can not generate any level operation under open-circuit fault condition of the capacitor.</li> <li>□ larger energy storage requirement.</li> </ul>

<p>[23]</p>		<p><math>N_{comp} = 10</math>  <math>TSV_{pu}/level = 4</math>  <math>gain = 2</math>  <math>T_{SC,M} = 1</math>  <math>\eta = 97.2\% @ 700</math>  <math>W</math></p>	<ul style="list-style-type: none"> <li><input type="checkbox"/> Can not generate any level operation under open-circuit fault condition of capacitor.</li> <li><input type="checkbox"/> low energy storage requirement.</li> </ul>
<p>[19]</p>		<p><math>N_{comp} = 11</math>  <math>TSV_{pu}/level = 2</math>  <math>gain = 1</math>  <math>T_{SC,M} = 1</math>  <math>\eta = 97.5\% @ 700</math>  <math>W</math></p>	<ul style="list-style-type: none"> <li><input type="checkbox"/> Can not generate any level operation under open-circuit fault condition of capacitor.</li> <li><input type="checkbox"/> Incapable of handling the <math>C_{R2}</math> failure.</li> <li><input type="checkbox"/> Lower energy storage requirement.</li> <li><input type="checkbox"/> Capable of handling the inductive load.</li> </ul>
<p>[24]</p>		<p><math>N_{comp} = 14</math>  <math>TSV_{pu} = 2</math>  <math>gain = 2</math>  <math>T_{SC,M} = 1</math>  <math>\eta = 96\% @ 700W</math></p>	<ul style="list-style-type: none"> <li><input type="checkbox"/> Can not generate any level operation under open-circuit fault condition of capacitor.</li> <li><input type="checkbox"/> Incapable of handling the <math>C_{R1}</math> failure.</li> <li><input type="checkbox"/> Lower energy storage requirement.</li> </ul>

[22]		$N_{\text{comp}} = 11$ $\text{TSV}_{\text{pu}} = 1.6$ $\text{gain} = 2$ $T_{\text{SC,M}} = 0.5$ $\eta = 94.23\% @ 70$ $0\text{W}$	<ul style="list-style-type: none"> <li><input type="checkbox"/> Can not generate any level operation under open-circuit fault condition of capacitor.</li> <li><input type="checkbox"/> Lower energy storage requirement.</li> </ul>
[21]		$N_{\text{comp}} = 13$ $\text{TSV}_{\text{pu/level}} = 1.66$ $\text{gain} = 1$ $T_{\text{SC,M}} = 0.5$ $\eta = 97.6\% @ 700$ $\text{W}$	<ul style="list-style-type: none"> <li><input type="checkbox"/> Can not generate any level operation under open-circuit fault condition of capacitor.</li> <li><input type="checkbox"/> Incapable of handling the <math>C_3</math> failure.</li> <li><input type="checkbox"/> Lower energy storage requirement.</li> </ul>
[P]		$N_{\text{comp}} = 6$ $\text{TSV}_{\text{pu/level}} = 0.7$ $\text{gain} = 2$ $T_{\text{SC,M}} = 1$ $\eta = 97.81\% @ 70$ $\text{W}$	<ul style="list-style-type: none"> <li><input type="checkbox"/> Can create a three-level when capacitor <math>C_1</math> and <math>C_2</math> are open-circuit.</li> <li><input type="checkbox"/> Lower energy storage requirement.</li> <li><input type="checkbox"/> Capable of handling the inductive load.</li> </ul>

## VI. Results Analysis

### (a) Results of the Simulation:

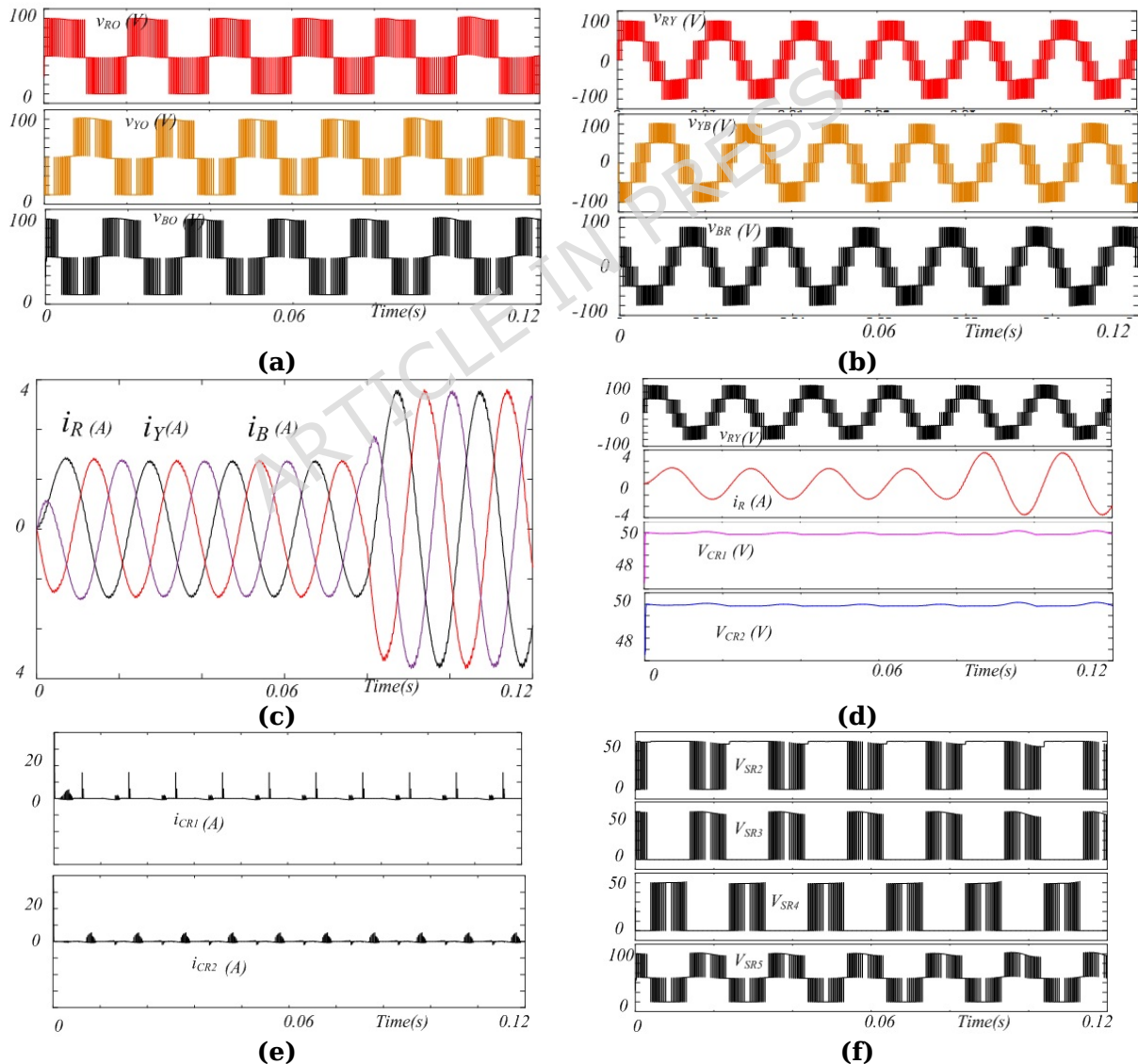
**Table 6: Parameters for Validation of Simulation and Experimentation**

Item	Specification
$V_{\text{DC}}$	50
$C_1, C_2$	2100 $\mu\text{F}$
$f_{\text{sw}}$	2000Hz
$f$	50 Hz
Diode	SBR40U300CTB, 300V, 40A
MOSFETs	IXTP36N30T(TO220), 300V, 36A
Driver	TLP250, 25kHz

load	R=50, L=80mH
------	--------------

\*www.mouser.in

A detailed time-domain simulation of the PT supplying an RL load has been performed to analyse its transient response. The system parameters are listed in Table 6. As illustrated in Fig. 7(a), the pole voltage waveform consistently exhibits three distinct levels of magnitude 50 V without distortion, even under varying load conditions. The corresponding line voltage waveforms of the PT are presented in Fig. 7(b), showing that a stable five-level (line to-line) output is maintained for each phase regardless of load variation. During transient states, the PT effectively adapts and maintains capacitor-voltage self-balancing under load variations, as demonstrated in Figs. 7(c). Fig. 7(d) illustrates the per-phase voltage, current, and capacitor voltage waveforms, providing a clearer understanding of the capacitor voltage balancing mechanism. Fig. 7(e) shows the current in capacitors. Fig. 7 (f) shows the voltage stress of various switches. Fig. 7 (g-h) shows the transient response of the input voltage and the modulation index. Fig. 7(i) and (j) show the total harmonic distortion (THD) of the voltage and current, respectively.



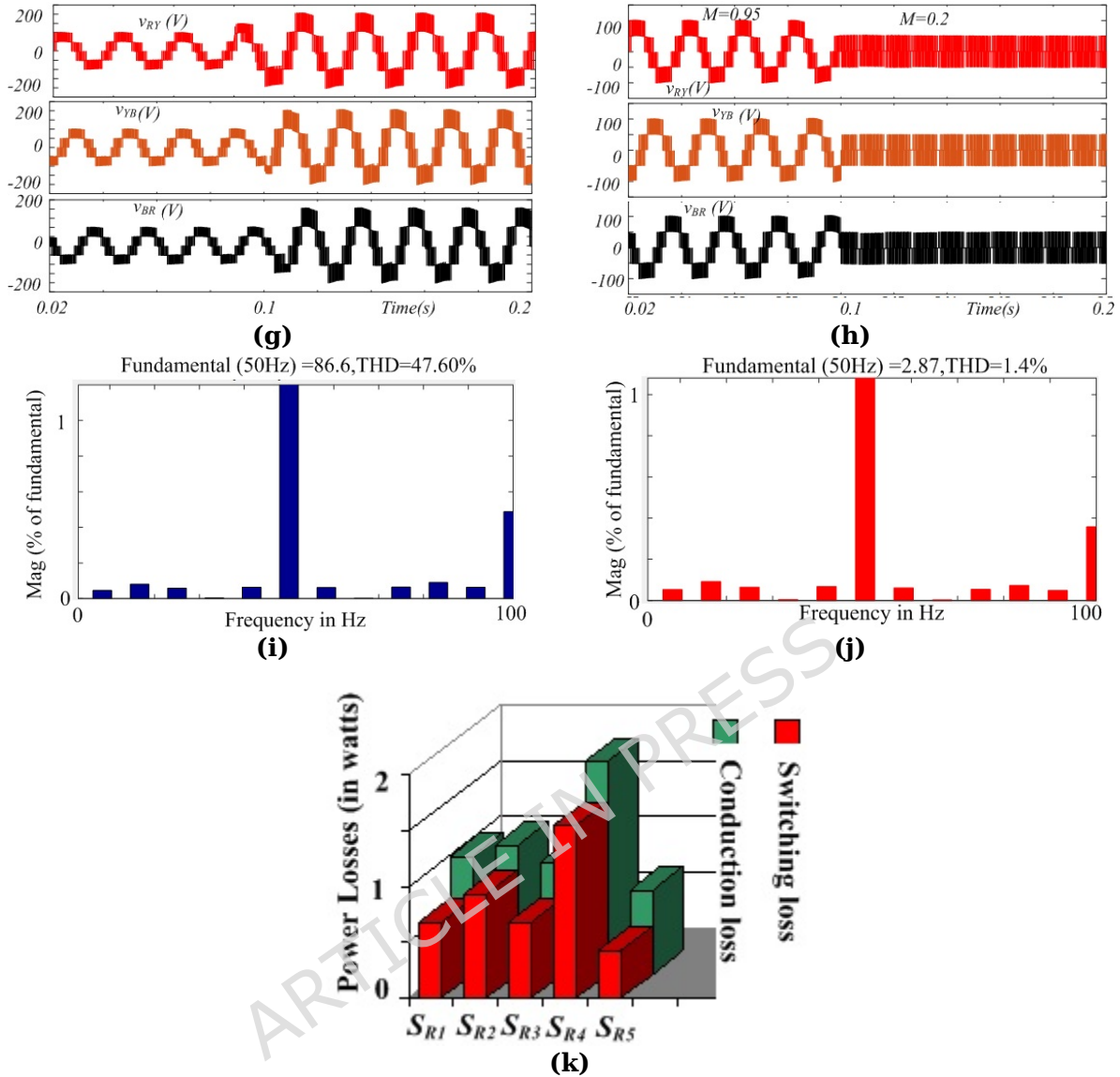
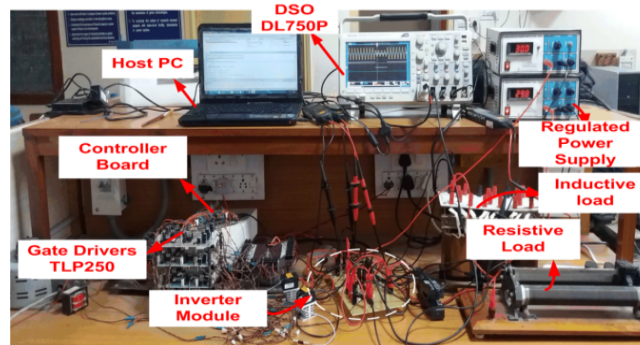


**Fig. 7** displays simulation results (a),  $v_{RO}$ ,  $v_{YO}$ ,  $v_{BO}$  (b)  $v_{RY}$ ,  $v_{YB}$ ,  $v_{BR}$ , (c)  $i_{iR}$ ,  $i_Y$ ,  $i_B$  (d) (d) Per Phase,  $v_{RY}$ ,  $i_R$ ,  $V_{CR1}$ ,  $V_{CR2}$  (e) capacitor charging current (f) voltage stress of the switches (g) step change in voltage (h) step change in modulation index (i) voltage THD (j) Current THD (k) loss distribution graph

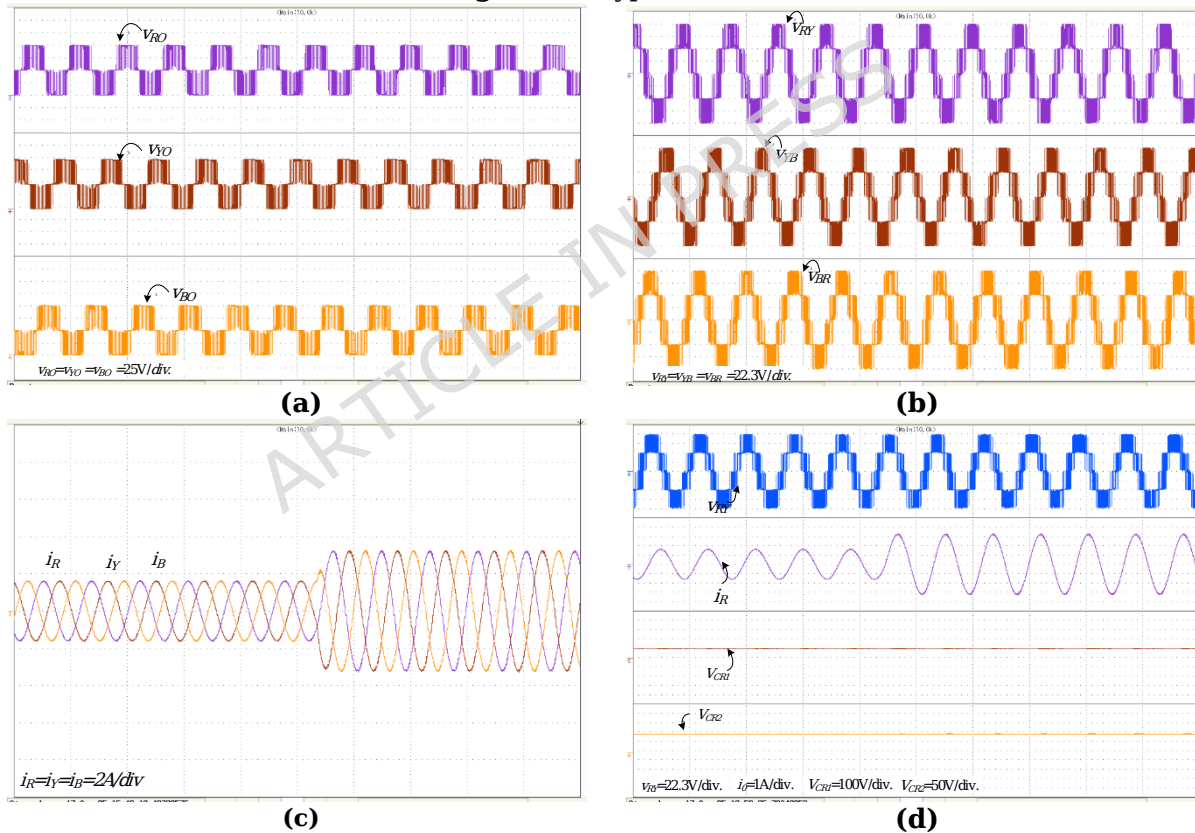
### (b) Results of the experiment:

To confirm the efficacy of the PT, experimental testing was performed in the laboratory. Table 6 shows the parameters used for the experimental setup, and Fig. 8 shows the laboratory prototype module. The corresponding experimental results are presented in Fig. 9. The PT makes a three-level pole voltage ( $v_{RO}$ ,  $v_{YO}$ ,  $v_{BO}$ ) and each level has the same amount of 50V, as shown in Fig. 9(a). Figure 9(b-c) shows the PT line voltages ( $v_{RY}$ ,  $v_{YB}$ ,  $v_{BR}$ ) and the line currents ( $i_R$ ,  $i_Y$ ,  $i_B$ ). It has been noted that the PT setup successfully creates a 5-level line-to-line voltage when the load is stepped in increments. Figure 9(d) shows the phase voltage and current waveforms during transient conditions, making it

easier to understand how the capacitor maintains its voltage. Fig. 9(e) displays the power and efficiency behaviors for both simulation and experimentation under different loading circumstances. Changes in voltage and modulation index are shown in Fig.9 (f-g), respectively. Voltage stress and capacitor current are shown in Fig.9(h-i). Approximately zero leakage current of the proposed structure is shown in Fig. 9(j), making it suitable for PV applications. Fig.9(k-l) shows the THD analysis of the proposed SCMLI.



**Fig.8** Prototype module



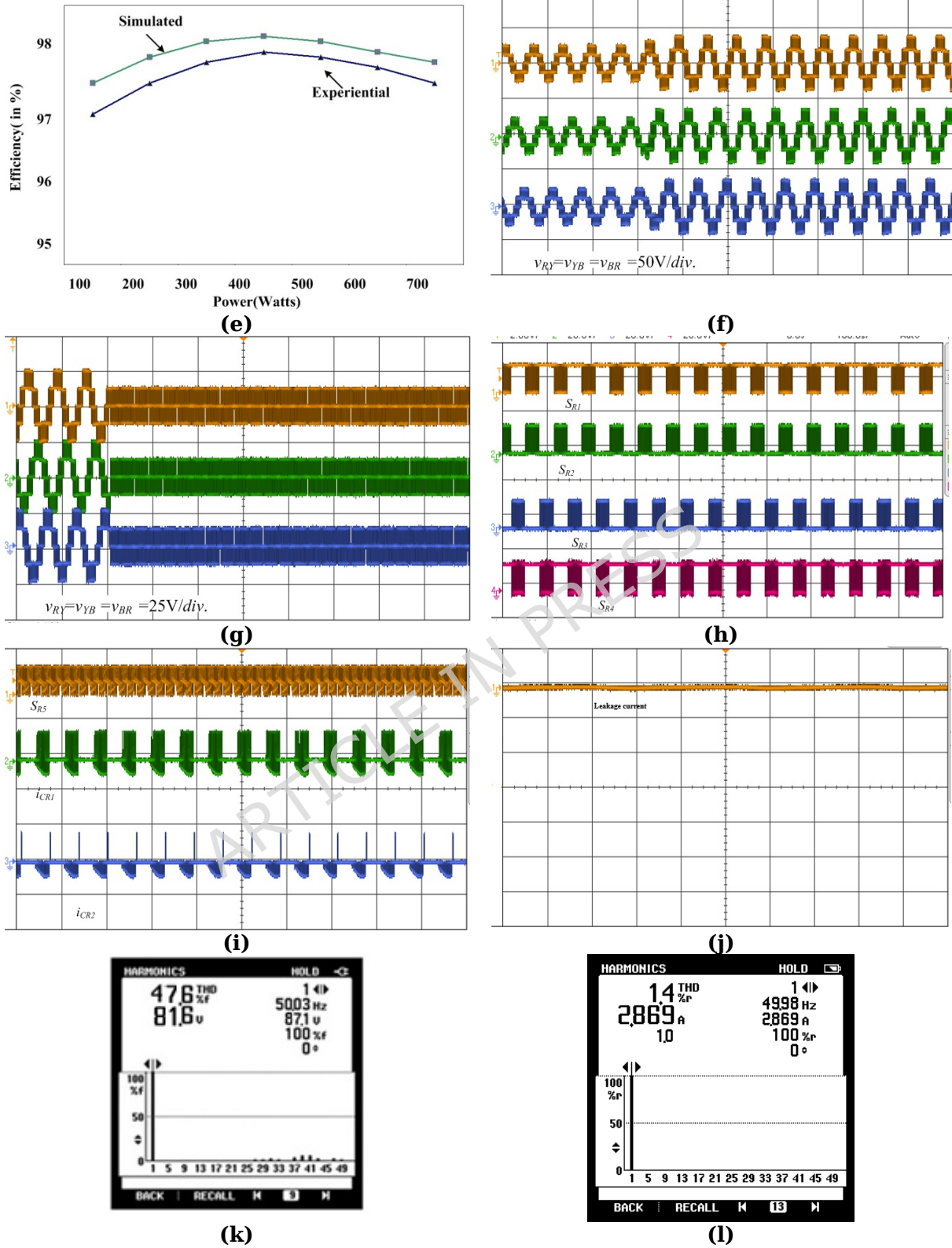


Fig.8 Experimental Results (a),  $v_{RO}$ ,  $v_{YO}$ ,  $v_{BO}$  (b)  $v_{RY}$ ,  $v_{YB}$ ,  $v_{BR}$ , (c)  $i_{iR}$ ,  $i_{YB}$  (d) Per Phase,  $v_{RY}$ ,  $i_R$ ,  $v_{CR1}$ ,  $v_{CR2}$  (e) Power Vs Efficiency curve (f) change in input voltage (g) change in Modulation index (h) voltage stress (i) capacitor current stress (j) leakage

current (k)Voltage THD (l) Current THD

## VII. Conclusion

A novel three-phase five-level SCMLI for RE applications is presented in this article. Additionally, the suggested inverter achieves capacitor self-balancing by eliminating the need for voltage sensors. It attains a voltage gain of two and a noteworthy least TSV of 7. Due to its boosting capability, the proposed SCMLI is suitable for applications in PV, EV, and UPS. A thorough comparison analysis demonstrates this topology superiority over current designs. A prototype module is used to experimentally validate the PT, confirming reliable operation across different operational modes. Moreover, the maximum efficiency of the PT is around 97.81% at 400 W and the cost is \$54.59.

### Declarations:

**Acknowledgement:** Not Applicable.

**Funding Statement:** The study was not supported by any grant.

**Authors' Contribution:** NN, KJ: Conceptualization, Methodology, Data Analysis, Writing-original draft. KJ, KKG: Visualization, Supervision, Validation. AMK, DK, NKD: Visualization, Analysis, Writing - review & editing.

**Data availability:** The datasets used and/or analyzed during the current study are available from the corresponding author upon reasonable request.

**Conflict of Interest declaration:** The authors declare that they have NO affiliations with or involvement in any organization or entity with any financial interest in the subject matter or materials discussed in this manuscript.

**Competing interest:** The authors declare that they have no known competing financial interests or personal relationships that could have appeared to influence the work reported in this paper.

**Ethical Approval:** Ethical and professional standards have been met. No animals or humans are used in this study.

## References

- [1] K. K. Gupta, A. Ranjan, P. Bhatnagar, L. K. Sahu and S. Jain, "Multilevel Inverter Topologies With Reduced Device Count: A Review," in *IEEE Transactions on Power Electronics*, vol. 31, no. 1, pp. 135-151, Jan. 2016, doi: 10.1109/TPEL.2015.2405012.
- [2] J. I. Leon, S. Vazquez and L. G. Franquelo, "Multilevel Converters: Control and Modulation Techniques for Their Operation and Industrial Applications," in *Proceedings of the IEEE*, vol. 105, no. 11, pp. 2066-2081, Nov. 2017, doi: 10.1109/JPROC.2017.2726583.
- [3] S. S. Lee, C. S. Lim, Y. P. Siwakoti and K. -B. Lee, "Dual-T-Type Five-Level Cascaded Multilevel Inverter With Double Voltage Boosting Gain," in *IEEE Transactions on*

- Power Electronics, vol. 35, no. 9, pp. 9522-9529, Sept. 2020, doi: 10.1109/TPEL.2020.2973666.
- [4] K. Jena, D. Kumar, K. Janardhan, B.H. Kumar, A.R Singh, S .Nikolovski, M. Bajaj "A Novel Three-Phase Switched-Capacitor Five-Level Multilevel Inverter with Reduced Components and Self-Balancing Ability" Applied Sciences. 2023; 13(3):1713. <https://doi.org/10.3390/app13031713>
- [5] A. Jakhar, N. Sandeep and A. K. Verma, "A Five-Level X-Type Boosting Inverter With Reduced Stored Energy of Switched-Capacitors," in IEEE Transactions on Circuits and Systems II: Express Briefs, vol. 71, no. 3, pp. 1476-1480, March 2024, doi: 10.1109/TCSII.2023.3325623.
- [6] M. S. Ahmed, R. Raushan and M. Waseem Ahmad, "A Reduced Capacitance H-9 Five-Level Switched Boost Capacitor Transformerless Inverter," in IEEE Transactions on Circuits and Systems II: Express Briefs, vol. 72, no. 5, pp. 788-792, May 2025, doi: 10.1109/TCSII.2025.3552764.
- [7] A. Jakhar and N. Sandeep, "Five-Level Common-Ground-Type Boosting Inverter With Lesser Capacitor-Stored Energy," in IEEE Transactions on Power Electronics, vol. 38, no. 12, pp. 15121-15125, Dec. 2023, doi: 10.1109/TPEL.2023.3314896.
- [8] P. R. Surapu, N. Sandeep and A. K. Verma, "Five-Level ANPC Inverter With Full DC-Bus Utilization," in IEEE Transactions on Power Electronics, vol. 39, no. 1, pp. 83-87, Jan. 2024, doi: 10.1109/TPEL.2023.3323794.
- [9] D. -T. Do, T. -T. Vu, K. M. Nguyen and V. -T. Tran, "A Single-Phase Five-Level Switched-Capacitor Boost Inverter With Improving Voltage Gain," in IEEE Access, vol. 13, pp. 67942-67951, 2025, doi: 10.1109/ACCESS.2025.3560985.
- [10] R. Barzegarkhoo, Y. P. Siwakoti, R. P. Aguilera, M. N. H. Khan, S. S. Lee and F. Blaabjerg, "A Novel Dual-Mode Switched-Capacitor Five-Level Inverter With Common-Ground Transformerless Concept," in IEEE Transactions on Power Electronics, vol. 36, no. 12, pp. 13740-13753, Dec. 2021, doi: 10.1109/TPEL.2021.3074517.
- [11] S. S. Lee, Y. P. Siwakoti, R. Barzegarkhoo and K. -B. Lee, "Switched-Capacitor-Based Five-Level T-Type Inverter (SC-5TI) With Soft-Charging and Enhanced DC-Link Voltage Utilization," in IEEE Transactions on Power Electronics, vol. 36, no. 12, pp. 13958-13967, Dec. 2021, doi: 10.1109/TPEL.2021.3088443.
- [12] K. Jena, C. K. Panigrahi,, K. K Gupta,, & D. Kumar, "A generalized transformerless switched-capacitor inverter for photovoltaic application" Electrical Engineering, vol.104, no.5, pp.3435-3444. Oct 2022 doi: <https://doi.org/10.1007/s00202-022-01496-6>
- [13] M. Saeedian, S. M. Hosseini and J. Adabi, "A Five-Level Step-Up Module for Multilevel Inverters: Topology, Modulation Strategy, and Implementation," in IEEE Journal of Emerging and Selected Topics in Power Electronics, vol. 6, no. 4, pp. 2215-2226, Dec. 2018, doi: 10.1109/JESTPE.2018.2819498.
- [14] A. Khodaparast, J. Adabi, and M. Rezanejad, "A step-up switchedcapacitor multilevel inverter based on 5-level T-type modules," IET Power Electron., vol. 12, no. 3, pp. 483-491, Mar. 2019.
- [15] M. N. H. Khan et al., "A Common Grounded Type Dual-Mode Five-Level Transformerless Inverter for Photovoltaic Applications," in IEEE Transactions on Industrial Electronics, vol. 68, no. 10, pp. 9742-9754, Oct. 2021, doi: 10.1109/TIE.2020.3028810.

- [16] S. Kumari, A. K. Verma, S. N, U. R. Yaragatti and H. R. Pota, "A Five-Level Transformer-Less Inverter With Self-Voltage Balancing and Boosting Ability," in *IEEE Transactions on Industry Applications*, vol. 57, no. 6, pp. 6237-6245, Nov.-Dec. 2021, doi: 10.1109/TIA.2021.3116222.
- [17] L. He and C. Cheng, "A Flying-Capacitor-Clamped Five-Level Inverter Based on Bridge Modular Switched-Capacitor Topology," in *IEEE Transactions on Industrial Electronics*, vol. 63, no. 12, pp. 7814-7822, Dec. 2016, doi: 10.1109/TIE.2016.2607155.
- [18] N. Sandeep, J. S. M. Ali, U. R. Yaragatti and K. Vijayakumar, "A Self-Balancing Five-Level Boosting Inverter With Reduced Components," in *IEEE Transactions on Power Electronics*, vol. 34, no. 7, pp. 6020-6024, July 2019, doi: 10.1109/TPEL.2018.2889785.
- [19] Y. P. Siwakoti, "A new six-switch five-level boost-active neutral point clamped (5L-Boost-ANPC) inverter," 2018 *IEEE Applied Power Electronics Conference and Exposition (APEC)*, San Antonio, TX, USA, 2018, pp. 2424-2430, doi: 10.1109/APEC.2018.8341356.
- [20] Y. Ye, S. Chen, R. Sun, X. Wang and Y. Yi, "Three-Phase Step-Up Multilevel Inverter With Self-Balanced Switched-Capacitor," in *IEEE Transactions on Power Electronics*, vol. 36, no. 7, pp. 7652-7664, July 2021, doi: 10.1109/TPEL.2020.3047198.
- [21] Y. Ye, T. Hua, S. Chen and X. Wang, "Neutral-Point-Clamped Five-Level Inverter With Self-Balanced Switched Capacitor," in *IEEE Transactions on Industrial Electronics*, vol. 69, no. 3, pp. 2202-2215, March 2022, doi: 10.1109/TIE.2021.3066932.
- [22] S. K. Dalai, K. P. Panda, Y. P. Siwakoti and G. Panda, "Three-Phase Switched-Capacitor Boost Self-Balanced Multilevel Inverter for Photovoltaic Applications," in *IEEE Transactions on Energy Conversion*, vol. 39, no. 3, pp. 1818-1827, Sept. 2024, doi: 10.1109/TEC.2024.3367733.
- [23] D. -T. Do, K. M. Nguyen and V. -T. Tran, "A Novel Three-Level Quasi-Switched Boost F-Type Inverter With High Voltage Gain and Self-Balanced Neutral-Point Voltage," in *IEEE Access*, vol. 11, pp. 34783-34794, 2023, doi: 10.1109/ACCESS.2023.3265081.
- [24] W. Zhang, H. Wang, X. Zhu, H. Wang, X. Deng and X. Yue, "A Three-Phase Five-Level Inverter With High DC Voltage Utilization and Self-Balancing Capacity of Floating Capacitor," in *IEEE Transactions on Power Electronics*, vol. 37, no. 9, pp. 10609-10619, Sept. 2022, doi: 10.1109/TPEL.2022.3163158.
- [25] S. K. Baksi, R. K. Behera and U. R. Muduli, "A Comprehensive Analysis of Enhanced DC-Bus Utilization and Reduced Component Count Five-Level Inverter for PV-Grid Integration," in *IEEE Transactions on Industry Applications*, vol. 61, no. 2, pp. 3303-3316, March-April 2025, doi: 10.1109/TIA.2025.3532231.
- [26] A. Taghvaie, J. Adabi and M. Rezanejad, "A Self-Balanced Step-Up Multilevel Inverter Based on Switched-Capacitor Structure," in *IEEE Transactions on Power Electronics*, vol. 33, no. 1, pp. 199-209, Jan. 2018, doi: 10.1109/TPEL.2017.2669377.
- [27] A. R. Hasouna, S. A. Mahmoud, A. E. El-Sabbe, Dina S.M. Osheba, "A 6X-3X voltage gain thirteen level switched capacitor based inverter with reduced switches count for low voltage sources" *Computers and Electrical Engineering*, Volume 130, 2026, doi.org/10.1016/j.compeleceng.2025.110864